Available online at www.sciencedirect.com
ScienceDirect
Surface Science 600 (2006) 3388–3393
SURFACE SCIENCE
www.elsevier.com/locate/susc

Active role of buried ultrathin oxide layers in adsorption of O_2 on Au films

Su Ying Quek [a], Cynthia M. Friend [a,b], Efthimios Kaxiras [a,c,*]

[a] Division of Engineering and Applied Sciences, Harvard University, Cambridge MA 02138, USA
[b] Department of Chemistry and Chemical Biology, Harvard University, Cambridge MA 02138, USA
[c] Department of Physics, Harvard University, Cambridge MA 02138, USA

Received 17 February 2006; accepted for publication 23 May 2006
Available online 27 June 2006

Abstract

Ultrathin oxide layers can exhibit special behavior by enabling the coupling of structural distortions and charge transfer beyond that allowed in the bulk. In this work, we show from first-principles calculations that ultrathin layers of titania, a prototypical oxide, are active in stabilizing adsorption of O_2 on Au overlayers. The adsorbed O_2 molecules induce charge redistribution in Au that penetrates to the Au–titania interface, which responds through structural distortions that lower the total energy of the system. We suggest that this effect may be of more general nature and useful in catalysis.

Keywords: Density functional calculations; Gold; Titanium oxide; Catalysis; Interfaces; Heterostructures and thin film structure

1. Introduction

Ultrathin oxide films have attracted immense interest because of their numerous technological applications [1]. In parallel development, oxide-supported metal nanostructures have been shown to be useful as sensors [2] and catalysts [3]. In particular, the oxide support can enhance the catalytic activity of the metal nanostructure by altering its electronic properties prior to catalysis, via charge transfer [4,5] and strain [6,7]. In this work, we propose that when the support is an ultrathin reducible oxide film, atoms at the buried metal-oxide interface can rearrange in response to the presence of adsorbates on the metal film, provided the latter is sufficiently thin. This atomic relaxation at the interface lowers the total energy of the system, thereby stabilizing adsorption. We call the ability of interfacial atoms to rearrange during adsorption 'dynamic interface fluxionality'. We demonstrate this effect on a model structure consisting of a thin Au film on an ultrathin titania layer supported on a molybdenum slab, and suggest that it will be of more general nature. Specifically, we expect that when the metal film forms strong covalent bonds with the reducible ultrathin oxide layer, while the latter does not interact strongly with its support to render it a rigid structure, dynamic interface fluxionality can take place. This effect may be exploited to design better catalysts and sensors by replacing traditional reducible oxide supports with ultrathin oxide films. Recent advances in the control of ultrathin film growth [8] indicate that this is a practical possibility.

An oxide/metal system that has attracted tremendous attention is that of oxide-supported Au nanoparticles and films, which act as excellent catalysts [9]. Theoretical studies indicate that the active sites include under-coordinated Au atoms [10,11] with rough orbitals [12], and sites at the Au-oxide interface [13,14]. Experiments also suggest that the activity of titania-supported Au films increases markedly when the Au thickness is reduced to one nearest neighbor distance in bulk Au (so-called 'bilayers') [15]. A key

* Corresponding author. Address: Department of Physics, Harvard University, 17 Oxford Street, Cambridge , MA 02138, USA. Tel.: +1 617 495 7977; fax: +1 617 496 2545.
E-mail address: kaxiras@physics.harvard.edu (E. Kaxiras).

0039-6028/$ - see front matter © 2006 Published by Elsevier B.V.
doi:10.1016/j.susc.2006.05.060

insight from theoretical studies was that the ability of Au atoms in a nanoparticle to rearrange in response to adsorbates is essential for O_2 adsorption [16]; this effect was called 'fluxionality' of the nanoparticle. Here, we show that the notion of fluxionality can be extended to the Au-oxide interface for ultrathin Au films on ultrathin reduced titania.

2. Motivation

The possibility of wetting an ultrathin titania support with Au films was recently demonstrated [15], with Mo(1 1 2) as a substrate on which the TiO_2 thin film was grown. CO oxidation activity in this system was >45 times greater than that reported for other Au/titania catalysts. The atomic structure of this system is unknown. However, two salient features are the strong interaction between Au and titania through Au–Ti bond formation, and the presence of ultrathin reduced titania beneath the Au film. Both of these effects have precedent in other systems [17,18]. Reducible oxides grown on a metal substrate have lower oxidation states than bulk phases due to the reducing character of the metal surface (in the present case, Mo) [17]. On bulk TiO_2 surfaces, Au binds almost exclusively to reduced Ti sites [18]. The availability of such sites throughout the ultrathin titania film thus allows wetting by Au. What is not clear, however, is how a strong interaction with buried ultrathin titania, or a small Au thickness, can enhance the activity of Au/titania catalysts [19].

Motivated by these questions, and knowledge [13,20] that the CO oxidation rate is limited by the availability of O_2 or adsorbed O on the catalyst, we study O_2 and O adsorption in a model ultrathin Au/titania system.

3. Choice of model

We first explain our choice of a structural model for this system. While this model may not be an exact representation of the experimental system (the atomic structure of which remains undetermined) it has been constructed by taking into account information from various experiments as well as from extensive simulations. More specifically, our model is motivated by the following observations.

Firstly, the substrate consists of a Mo(1 1 2) surface, which has a row-and-trough structure that makes it a useful substrate for ultrathin oxide growth. It has been proposed that the oxide grows along the troughs, forming O–Mo bonds [21]. Our simulations confirm that this is energetically preferred.

Secondly, assuming that the Ti and Mo have the same periodicity along the troughs (as suggested by LEED experiments) leads to an interface structure in which the Ti atom positions are compatible with a Au(1 1 0) lattice strained by 9.1% and −5.5% in the [0 0 1] and [1 $\bar{1}$ 0] directions, respectively. Au(1 1 0) layers, with strains of 12.5% and −7.5% along these directions, have previously been grown on anatase TiO_2(1 1 0) up to length-scales of at least 4 nm and thicknesses of at least four layers, as shown by high resolution transmission electron microscopy [22]. Thus, with suitable growth procedures, it is plausible that the titania/Mo system can support 1 or 2 Au(1 1 0) layers over length-scales significantly greater than 4 nm. We determined the most stable such structure, shown in Fig. 1, by exploring 37 distinct initial geometries.

Thirdly, although the Ti:O stoichiometry in this favored structure is 1:2, the oxide is not fully oxidized since O is bonded to strongly-reducing Mo. The oxide atoms are arranged in a motif present on rutile TiO_2(1 1 0), the most stable crystal face of TiO_2.

Fourthly, each titania row corresponds to a row of bridging O vacancies on this surface. Such vacancies are common and can form complete rows [23]. Au can nucleate at these vacancies [18], forming Au–Ti bonds in a similar geometry as in our model [23].

We refer to the structures with 1 and 2 Au(1 1 0) layers, which consist of 3 and 5 distinct planes of Au atoms on the oxide layer, respectively, as titania/Au_3 (shown in Fig. 1(a)–(b)) and titania/Au_5 (shown in Fig. 1(c)).

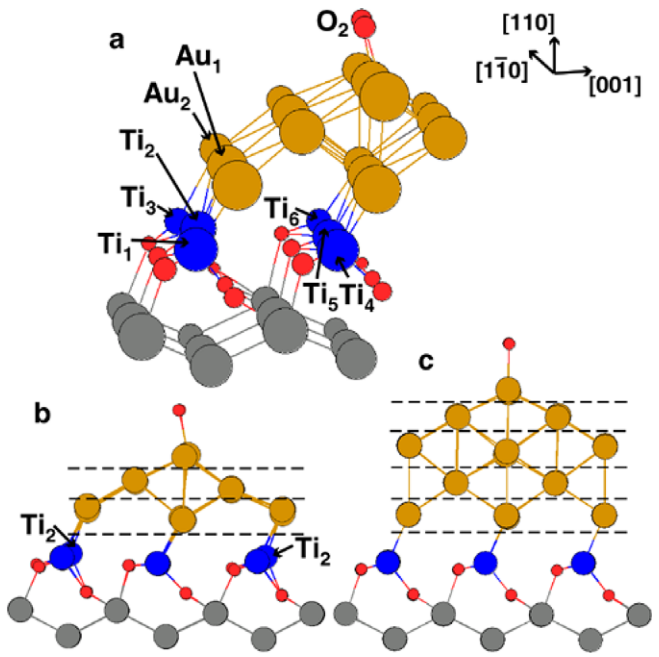

Fig. 1. (a) O_2 adsorbed on titania/Au_3. (b) View of (a) down the [1 $\bar{1}$ 0]-direction. (c) O_2 adsorbed on titania/Au_5. Red, blue, gold and gray circles denote O, Ti, Au and Mo respectively. Only the top two layers of the Mo slab are shown. Crystallographic directions corresponding to those of the Au layers are indicated. Dashed lines separate the Au(1 1 0) films into 3 Au planes in titania/Au_3, and 5 in titania/Au_5. On the clean Au surface, all atoms are equivalent by periodicity in the [1 $\bar{1}$ 0]-direction; Ti rows directly beneath the troughs of the Au(1 1 0) layers are also equivalent by periodicity. Thus, calculations with the clean Au surface have two Ti atoms per unit cell. For calculations with adsorbates, the period in the [1 $\bar{1}$ 0]-direction of Au(1 1 0) is tripled; inequivalent atoms at the interface after O_2 adsorption are labeled for reference in the text. (For interpretation of the references in colour in this figure legend, the reader is referred to the web version of this article.)

4. Computational details

To investigate the adsorption process on this model system, we have performed first-principles calculations based on density functional theory (DFT) as implemented in VASP [24]. We used the projected augmented wave method with the generalized gradient approximation for the exchange-correlation functional (PW-91) and scalar relativistic pseudopotentials to represent the atomic cores. The Mo substrate was modeled by a 6-layer slab. The bottom 3 Mo layers were held fixed at their bulk positions, and all other atoms were relaxed until the atomic forces were smaller in magnitude than 0.05 eV/Å. The vacuum region separating slabs was taken to have thickness of $\geqslant 11$ Å, and reciprocal space sampling was performed on a k-point mesh of 6×12 per (1×1) Mo(1 1 2) surface unit cell; these computational parameters ensure adequate accuracy in the reported values, as determined by careful convergence studies. Spin-polarization was included in calculating the energies of structures involving O_2 molecules.

5. Results and discussion

Fig. 1 shows O_2 adsorbed at its most favorable site (involving under-coordinated Au atoms) in a 'top-bridge-top' geometry. This is consistent with other DFT studies of O_2 adsorption on Au surface steps [6] and Au clusters [12,25]. Adsorption of O_2 is accompanied by a charge transfer from Au to the O_2 unoccupied anti-bonding orbitals. The adsorption energies are -0.18 eV in titania/Au_3 and -0.03 eV in titania/Au_5. At other sites, this energy is positive, indicating repulsive interactions. It is likely that O_2 adsorbs more strongly than predicted by these values, because the calculated bond enthalpy of isolated O_2 molecules is -6.65 eV, while the experimentally measured value is -5.25 eV [26]; in other words, the reference configuration for adsorption energies, with the O_2 molecule far from the surface, is disproportionally favored due to the overestimation of the molecular bond enthalpy, as is common in DFT calculations of the type reported here [26]. We note, however, that all subsequent discussion and conclusions are based entirely on relative adsorption energies, which are well-described by DFT and are not affected by this problem.

In titania/Au_3, O_2 adsorption causes the bonds between the pairs of atoms Au_2–Ti_2 and Au_1–Ti_2 to shorten by 2.2% and 2.5%, and those between the pairs Au_2–Ti_3 and Au_1–Ti_1 to lengthen by 5.8% and 6.2%. No such distortion is observed in titania/Au_5, where the Au–Ti bond lengths change by less than 1.1% upon O_2 adsorption. When the titania/Mo support and Au atoms in contact with it are held fixed, the adsorption energy in titania/Au_3 becomes -0.04 eV, 0.14 eV higher than the value with full relaxation. The corresponding energy change in titania/Au_5 is only 0.01 eV. Thus, the interface distortion observed in titania/Au_3 plays a major role in stabilizing O_2 adsorption.

The different behavior of the two structures could be due to several factors. One possibility is the difference in densities of states (DOS) near the Fermi level, projected onto the Ti atoms. However, the Ti-projected DOS are similar in the two systems (Fig. 2). The absence of interface distortions in titania/Au_5 is therefore likely to be due to the thicker Au film. This may be related to the relative stability of titania/Au_5 compared to titania/Au_3: the thicker Au film in titania/Au_5 results in a larger cohesive energy, although actual relative stabilities will have to be evaluated by including a chemical potential for Au that is appropriate for the growth conditions. Analysis of the charge density distribution also shows that the thicker Au film effectively screens the buried interface from the effect of O_2 adsorption. Specifically, charge density difference plots show that charge transfer to O_2 induces a charge redistribution between the Au planes that is inhomogeneous in the $[1\,\bar{1}\,0]$-direction, but the inhomogeneity disappears for $n \geqslant 3$ in titania/Au_5 (Fig. 3). O_2-induced charge inhomogeneity in Au is thus screened out beyond a depth of approximately 3Å (one nearest-neighbor distance in bulk Au) below O_2, which corresponds to about 3 Au planes in titania/Au_5. To quantify this effect, we use the Bader method [27] to evaluate the charge contribution to O_2 from each Au plane in the films (Fig. 1). Unlike Mulliken charge assignments, the Bader method is independent of the choice of basis. The charge contribution from the nth Au plane beneath O_2 decreases exponentially with n, with zero contribution from the 5th plane beneath O_2 in titania/Au_5 (Table 1). Titania beneath the thicker Au film is thus insensitive to the O_2 adsorption geometry, precluding O_2-induced structural distortions at the interface. In contrast, the Au–titania interface in titania/Au_3 can distort in response to charge inhomogeneity in the $[1\,\bar{1}\,0]$-direction.

Au interacts with titania by forming predominantly covalent bonds with Ti, as reported in previous studies [23,28]. The interface distortion in titania/Au_3 is accompanied by a marked increase in covalency between the atom labeled Ti_2 and its nearest Au neighbors. Correspondingly, O_2 adsorption results in a 0.14e increase in charge on atom Ti_2 in titania/Au_3. In contrast, the Ti charges in titania/Au_5 do not change by more than 0.01e. The O_2-induced interface distortions in titania/Au_3 are therefore related to changes in the Au–Ti bonding.

This change in Au–Ti bonding is related to the reducibility of titania. In reducible oxides, the occupation of valence metal d-orbitals can change with little energy cost. As on bulk TiO_2 surfaces, vacancy-induced states in our models have Ti 3d character. In TiO_2(1 1 0), these states appear in the band-gap of the oxide [29]. In our models, the concentration of vacancies is so high that Ti 3d states occur at the Fermi level. The energy cost to alter the Au–Ti bonding by changing the occupation of Ti 3d orbitals is therefore negligible. This picture should be contrasted to that of Au interacting with vacancies on irreducible oxides such as alumina. In the latter case, the simple metal Al easily loses all its valence electrons to its neighbors, forming a

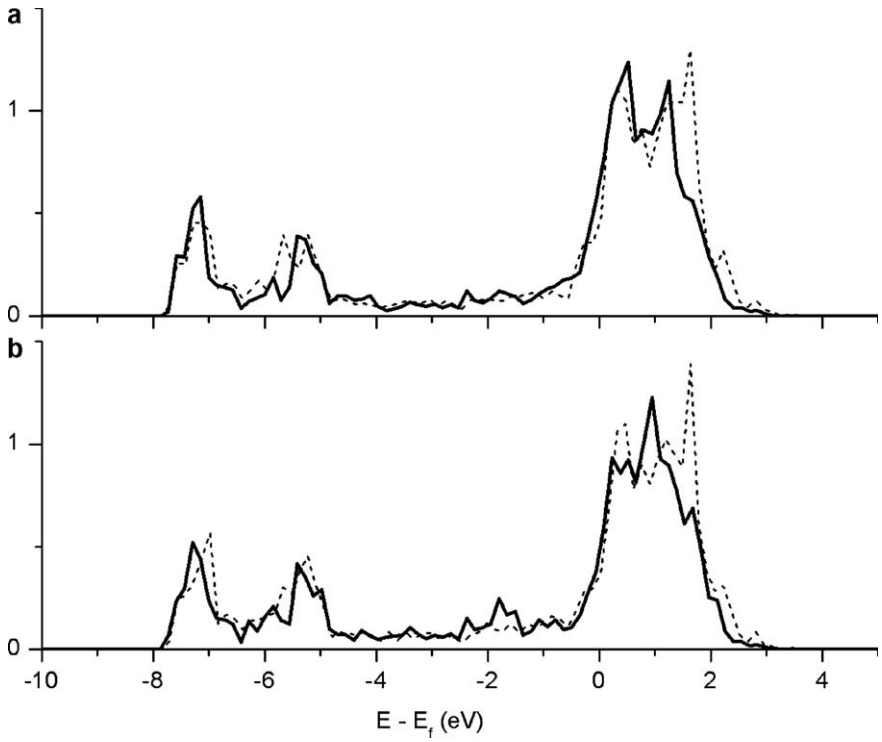

Fig. 2. Projected densities of states (DOS) on Ti atoms directly beneath the Au layers: (a) Ti atoms in Au troughs (labeled Ti_1, Ti_2, Ti_3 in Fig. 1(a)); (b) Ti atom in Au bridges (labeled Ti_4, Ti_5, Ti_6 in Fig. 1(a)), in titania/Au_3 (solid lines) and titania/Au_5 (dashed lines), for systems without adsorbates. DOS are in units of number of states per unit energy per unit cell, and are projected onto spherical harmonics centered on the Ti atoms (within spheres of radii 1.323 Å), summed over s, p and d contributions. The DOS close to the Fermi levels (E_f) are very similar in the two systems.

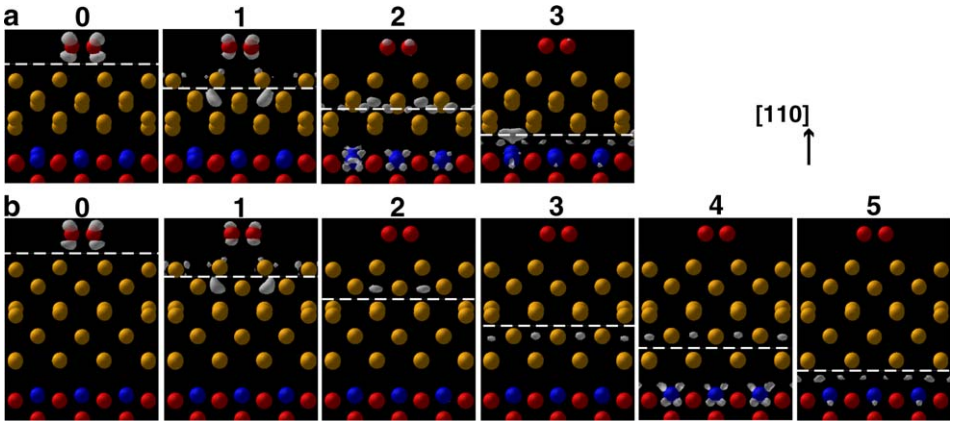

Fig. 3. Charge density difference isocontours (pale gray) for O_2 adsorbed on (a) titania/Au_3 and (b) titania/Au_5. Atoms are shown with the same symbols as in Fig 1 (the Mo substrate is not shown). The systems are viewed down the [0 0 1]-directions. The charge density difference is calculated by splitting the systems into two components: (i) the adsorbed O_2 on *n* Au planes, and (ii) the remaining Au planes and the titania/Mo support; the charge difference is between superposition of the two components (separated by a dashed white line in each panel) each considered separately and the entire system. Each panel is labeled by *n*, the number of Au planes in the first component, which ranges from 0 to 3 for titania/Au_3 and from 0 to 5 for titania/Au_5.

stable closed shell ion, Al^{3+}. It would be energetically unfavorable for Al^{3+} to change its electronic configuration during catalysis. To check this hypothesis, we have performed calculations using the same types of structures shown in Fig. 1, with Ti replaced by Al. As expected, we find no O_2-induced interface distortion in the alumina/Au structures.

The adsorption of individual O atoms on titania/Au_3 also induces stabilizing interface distortions. Fig. 4(a) shows O adsorbed at the two most stable sites (out of a total six sites that we have considered). As in O_2 adsorption, the most favorable adsorption site (P) involves undercoordinated Au atoms. The adsorption of individual H on the Au film, relevant to hydrogenation reactions in

Table 1
Charge gained (in e) per O_2

	1	2	3	4	5	Titania/Mo	**Total**
Titania/Au_3	0.31	0.12	0.03	–	–	0.05	0.51
Titania/Au_5	0.32	0.10	0.04	0.01	0.00	0.04	0.51

Column n gives the charge gained by O_2 from the nth Au plane beneath O_2, calculated by subtracting the charge on O_2 when it is attached to n planes, from the corresponding charge with $(n-1)$ planes. Values in column n are ≈3× those in column $n+1$. The titania/Mo support contributes charge to O_2 by changing the overall Au charge.

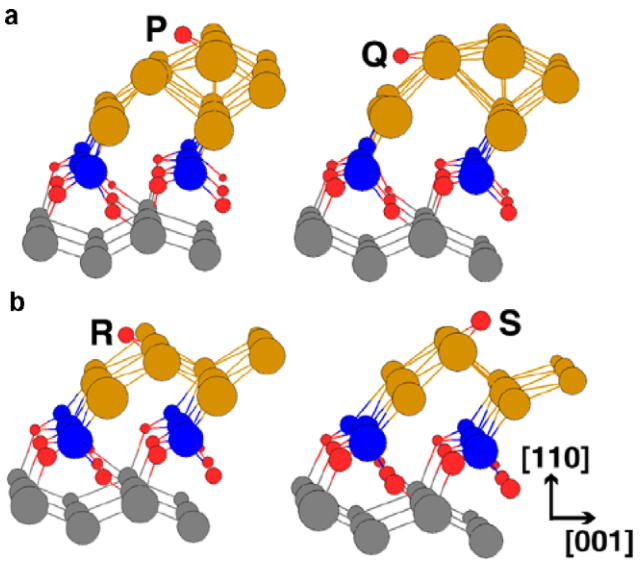

Fig. 4. O adsorbed in (a) titania/Au_3 and (b) titania/Au_2. We show adsorption at the 2 most stable sites in each case, out of a total of 6 sites considered in (a) and 4 in (b).

Au catalysis [30], also induces similar interface distortions. This shows that the ability to induce such distortions in titania/Au_3 is not limited to O_2. These general observations are quantified by detailed analysis of the energetics and structural distortions of the relevant structures, given in Table 2.

When the titania/Mo support and Au atoms in contact with it are held fixed, the local adsorbate-Au geometry remains similar, but the adsorption energy diminishes in titania/Au_3. The differences dE_{relax} in energies between the fully relaxed and constrained systems are 0.19 and 0.13 eV for O at the sites P and Q, and 0.10 eV for H at site P; this energy is 0.14 eV for adsorption of O_2, as discussed earlier. As a point of comparison, DFT studies have shown that O adsorption is 0.16 eV more stable on step defects than on a flat Au(1 1 1) surface [7]. The values of dE_{relax} are therefore significant in stabilizing adsorption. Table 2 also summarizes the adsorption-induced changes in bond lengths and Ti charges. In titania/Au_3, the maximum change in Ti charge, $d\rho_{max}$, varies from 0.09e to 0.15e and the maximum change in bond length, $dl(\text{Au–Ti})_{max}$, from +5.1% to +6.2%. Values of $dl(\text{Au–Au})_{max}$, the maximum change in Au–Au bond lengths, are significant, ranging from

Table 2
Adsorption in (a) titania/Au_5, (b) titania/Au_3 and (c) titania/Au_2

	BE (eV)	dE_{relax} (eV)	$d\rho_{max}$ (e) [site]	$dl(\text{Au–Ti})_{max}$ (%)	$dl(\text{Au–Au})_{max}$ (%)
(a) Titania/Au_5					
O_2	−0.03	0.01	–	1.2 (0.0)	7.7 (3.9)
(b) Titania/Au_3					
O_2	−0.18	0.14	0.14 [Ti_2]	6.2 (0.0)	−13.1 (−10.8)
O (P)	−3.56	0.19	0.15 [Ti_1]	6.2 (0.0)	−12.5 (13.1)
O (Q)	−3.43	0.13	0.09 [Ti_3]	5.7 (0.0)	19.8 (13.9)
H (P)	−2.26	0.10	0.11 [Ti_2]	5.1 (0.0)	−11.1 (6.7)
(c) Titania/Au_2					
O (R)	−3.40	0.07	−0.03 [Ti_3]	−1.5 (0.0)	8.9 (6.7)
O (S)	−3.34	0.25	0.12 [Ti_2]	11.0 (0.0)	6.8 (12.0)
H	−2.25	0.11	0.05 [Ti_2]	5.8 (0.0)	5.8 (5.8)

BE is the adsorption energy with respect to the isolated adsorbate and clean surface. dE_{relax}, $d\rho_{max}$, $dl(\text{Au–Ti})_{max}$ and $dl(\text{Au–Au})_{max}$ are described in the text. Values in brackets in columns $dl(\text{Au–Ti})_{max}$ and $dl(\text{Au–Au})_{max}$ are the corresponding changes obtained when the Ti atoms and Au atoms in contact with them are held fixed during adsorption. As $d\rho_{max}$ is within 0.02e in all constrained relaxations, only values of $|d\rho_{max}| > 0.02e$ are given, with the corresponding Ti sites in square brackets (using the labeling scheme of Fig. 1(a)).

−13.1% to 19.8%. This is expected since the adsorbates are directly adsorbed onto the Au films, and similar changes in Au–Au bond lengths are also observed in the constrained relaxations (given in brackets in Table 2).

An important consideration is to what extent the Au film structure assumed in our model influences the results. In order to assess this, we considered a different model, referred to as titania/Au_2, in which the top row of Au atoms from the titania/Au_3 structure has been removed (shown in Fig. 4(b)). The resulting Au film is a (1×1) Au(1 1 0) monolayer, in contrast to the (2×1) Au(1 1 0) films in titania/Au_3 and titania/Au_5. The latter films have a surface reconstruction that is characteristic of bulk Au(1 1 0) but may be unnecessary for Au(1 1 0) monolayers. Overall, adsorption of single O atoms has similar effects on interface distortions and charge transfer in titania/Au_2 as in titania/Au_3 as seen from the relevant quantities in Table 2. In the case of H atom adsorption, interface distortions at the most favorable site in titania/Au_2 are significant and comparable to those in titania/Au_3.

6. Concluding remarks

Larger adsorption energies have implications for catalysis because the availability of adsorbed reactants is a major rate-limiting factor for Au-based catalysts [7]. We have shown that interface fluxionality is essential in promoting adsorption of O_2 on ultrathin Au layers supported on ultrathin titania, and that this effect is lost when the metal layers become thicker. Further studies, involving larger scale simulations that incorporate dynamical and kinetic effects, are required to access the stability of these films under reaction conditions. This stability has implications for the lifetime of catalysts and sensors, and is known to be

a major problem for catalysts utilizing Au nanoparticles, which deactivate over time through agglomeration [31].

Our results are promising in the context of recent experimental advancements in the growth of ultrathin nanostructures on surfaces. For example, metastable nanostructures of reducible oxides have been grown on metal surfaces [17], and the reducing character of the metal substrate helps create active vacancy sites across the supported ultrathin oxide [17], which can allow wetting by transition metal catalysts [15]. The oxidation state of supported oxide nanostructures can also be tailored, in two-dimensional titania nanostructures on Au(111), for example [32]. Such oxide nanostructures and ultrathin films are likely to have much more flexibility to distort in response to adsorbates, compared to bulk oxide supports. The control of the features of nanostructures on substrates that can exhibit interface-fluxionality suggests that improved catalysts and sensors can be designed by replacing traditional reducible oxide supports by ultrathin oxide films.

Acknowledgements

We thank D.W. Goodman, M.S. Chen and B.K. Min for initial communications that motivated this work. S.Y.Q. thanks A-STAR, Singapore, for fellowship support. This work was partially supported by NCSA under DMR040002.

References

[1] M. Fernandez-Garcia, A. Martinez-Arias, J.C. Hanson, J.A. Rodriguez, Chem. Rev. 104 (2004) 4063.
[2] R.J. Wu, C.H. Hu, C.T. Yeh, P.G. Su, Sensor Actuat. B Chem. 96 (2003) 596.
[3] P.L. Gai, R. Roper, M.G. White, Curr. Opin. Solid. St. M 6 (2002) 401.
[4] B. Yoon, H. Hakkinen, U. Landman, A.S. Worz, J.M. Antonietti, S. Abbet, K. Judai, U. Heiz, Science 307 (2005) 403.
[5] Z.P. Liu, S.J. Jenkins, D.A. King, Phys. Rev. Lett. 94 (2005) 196102.
[6] Y. Xu, M. Mavrikakis, J. Phys. Chem. B 107 (2003) 9298.
[7] M. Mavrikakis, P. Stoltze, J.K. Nørskov, Catal. Lett. 64 (2000) 101.
[8] S.A. Chambers, Surf. Sci. Rep. 39 (2000) 105;
C.T. Campbell, Surf. Sci. Rep. 27 (1997) 1.
[9] M. Haruta, S. Tsubota, T. Kobayashi, H. Kageyama, M.J. Genet, B. Delmon, J. Catal. 144 (1993) 175.
[10] I.N. Remediakis, N. Lopez, J.K. Nørskov, Angew. Chem. Int. Edit. 44 (2005) 1824.
[11] N. Lopez, T.V.W. Janssens, B.S. Clausen, Y. Xu, M. Mavrikakis, T. Bligaard, J.K. Nørskov, J. Catal. 223 (2004) 232.
[12] G. Mills, M.S. Gordon, H. Metiu, J. Chem. Phys. 118 (2003) 4198.
[13] Z.P. Liu, X.Q. Gong, J. Kohanoff, C. Sanchez, P. Hu, Phys. Rev. Lett. 91 (2003) 266102.
[14] L.M. Molina, M.D. Rasmussen, B. Hammer, J. Chem. Phys. 120 (2004) 7673.
[15] M.S. Chen, D.W. Goodman, Science 306 (2004) 252.
[16] H. Hakkinen, W. Abbet, A. Sanchez, U. Heiz, U. Landman, Angew. Chem. Int. Edit. 42 (2003) 1297.
[17] S. Surnev, G. Kresse, M.G. Ramsey, F.P. Netzer, Phys. Rev. Lett. 87 (2001) 086102.
[18] E. Wahlstrom, N. Lopez, R. Schaub, P. Thostrup, A. Ronnau, C. Africh, E. Laegsgaard, J.K. Nørskov, F. Besenbacher, Phys. Rev. Lett. 90 (2003) 026101.
[19] C.T. Campbell, Science 306 (2004) 234.
[20] V.A. Bondzie, S.C. Parker, C.T. Campbell, Catal. Lett. 63 (1999) 143.
[21] M.S. Chen, W.T. Wallace, D. Kumar, Z. Yan, K.K. Gath, Y. Cai, Y. Kuroda, D.W. Goodman, Surf. Sci. 581 (2005) L115.
[22] S. Giorgio, C.R. Henry, B. Pauwels, G. Van Tendeloo, Mat. Sci. Eng. A Struct. 297 (2001) 197.
[23] N. Lopez, J.K. Nørskov, T.V.W. Janssens, A. Carlsson, A. Puig-Molina, B.S. Clausen, J.D. Grunwaldt, J. Catal. 225 (2004) 86.
[24] P.E. Blochl, Phys. Rev. B 50 (1994) 17953;
J.P. Perdew, Y. Wang, Phys. Rev. B 45 (1992) 13244;
G. Kresse, J. Furthmuller, Phys. Rev. B 54 (1996) 11169.
[25] A. Sanchez, S. Abbet, U. Heiz, W.D. Schneider, H. Hakkinen, R.N. Barnett, U. Landman, J. Phys. Chem. A 103 (1999) 9573.
[26] J.P. Perdew, K. Burke, M. Ernzerhof, Phys. Rev. Lett. 77 (1996) 3865.
[27] R.F.W. Bader, Atoms in Molecules-A Quantum Theory, Oxford University Press, New York, 1990;
G. Henkelman, A. Arnaldsson, H. Jónsson, Comput. Mat. Sci. 36 (2006) 254.
[28] J.A. Rodriguez, G. Liu, T. Jirsak, J. Hrbek, Z.P. Chang, J. Dvorak, A. Maiti, J. Am. Chem. Soc. 124 (2002) 5242.
[29] J.A. Rodriguez, J. Hrbek, Z. Chang, J. Dvorak, T. Jirsak, A. Maiti, Phys. Rev. B 65 (2002) 235414.
[30] G.C. Bond, D.T. Thompson, Catal. Rev. Sci. Eng. 41 (1999) 319.
[31] M. Valden, X. Lai, D.W. Goodman, Science 281 (1998) 1647.
[32] J. Biener, E. Farfan-Arribas, M. Biener, C.M. Friend, R.J. Madix, J. Chem. Phys. 123 (2005) 094705.